FIFTH INTERNATIONAL CONGRESS ON SOUND AND VIBRATION
DECEMBER 15-18, 1997
ADELAIDE, SOUTH AUSTRALIA

Specialist Keynote Paper

APPLICATION OF HARMONIC WAVELETS TO TIME-FREQUENCY MAPPING

DAVID E. NEWLAND

Department of Engineering
University of Cambridge
Trumpington Street
CAMBRIDGE
CB2 1PZ, UK
Email: den@eng.cam.ac.uk

ABSTRACT

Harmonic wavelets have simple formulations in the frequency domain and they have proved a good basis for the time-frequency mapping of transient signals. Moreover their computational algorithm allows bandwidth to be chosen arbitrarily so that they offer a variable Q transform, where Q is the ratio of centre frequency to bandwidth. In contrast, the short-time Fourier transform and the Wigner-Ville frequency decomposition method are constant bandwidth transforms, so that Q increases as frequency rises.

Although properties of wavelet orthogonality may be used to permit easy retrieval of the input signal, to achieve a high-definition time-frequency map more data is required than that obtained from a single decomposition of the input signal. This is achieved by repeating the frequency decomposition for different, overlapping bandwidths in order to increase the number of points that can be plotted.

Because bandwidth can be chosen arbitrarily, a frequency zoom feature can be incorporated into the harmonic wavelet transform algorithm. Also, because harmonic wavelets are complex, with real and imaginary parts, phase variations can be studied. Local changes in the spectral composition of a signal can be recognised, using either wavelet amplitude or phase as the discriminator. Examples of frequency zoom and of segmentation by amplitude and phase are given below. They demonstrate that the complex harmonic wavelet transform offers a computationally-efficient method of signal decomposition. Its principal advantage over the STFT is its variable Q property which becomes important when large amounts of data have to be processed.

THE HWT ALGORITHM FOR TIME-FREQUENCY MAPPING

Frequency versus time decomposition is possible by the short-time Fourier transform (STFT) and the Wigner-Ville method. The application of the first method is common and it offers a practical and conceptually simple route for time-frequency analysis. Its disadvantage is that it produces frequency coefficients for harmonics uniformly spaced across the whole frequency spectrum. For example, if an N point (real) time series is decomposed by the FFT there will be $N/2$ complex frequency coefficients covering the range from zero to the *Nyquist* frequency. Each harmonic is a constant frequency step from the last, so that the frequency interval is $Nyquist/(N/2)$. This means that to achieve close frequency resolution at the low frequency end of the spectrum, many high frequency harmonics have to be computed.

The Wigner-Ville method of analysis is an alternative method (see, for example, Cohen, 1995) which relies on the result that the spectral density of a signal is the Fourier transform of its autocorrelation function. For a stationary random process, autocorrelation is a function only of the separation time τ and then spectral density is independent of absolute time t. But for a transient signal, frequency composition changes with time and autocorrelation is a function of τ and t. Then spectral density is a function of absolute time t. Its amplitude is a measure of the distribution of energy over frequency and time. In practice there are complications due to the cross-terms that occur when two or more distinct frequencies interfere with each other because of the squaring operation involved in computing the second-order correlation function $x(t)x(t+\tau)$ (Mark, 1970). There are various ways of overcoming or at least greatly reducing this effect (Cohen, 1995; Hammond (ed), 1997) but there are two drawbacks. One is the high computational effort needed to compute the smoothed Wigner-Ville distribution. The other is the consequence of using an FFT computation to find the Fourier transform of the correlation function. As for the STFT this computes frequency components that are uniformly spaced on the frequency scale, so that to achieve acceptable resolution at low frequency, an excessively large number of harmonics may have to be computed at high frequency.

The harmonic wavelet transform is illustrated in figure 1 (from Newland, 1997a).

This makes the calculation

$$a(t) = \int_{-\infty}^{\infty} f(\tau)\, w^*(\tau - t)\, \mathrm{d}\tau . \qquad (1)$$

Knowledge of the wavelet coefficient $a(t)$ provides information about the structure of the input signal $f(t)$ and its relationship to the shape of the analysing wavelet $w(t)$. Because we are allowing for all the quantities to be complex, $w^*(t)$ the complex conjugate of $w(t)$ appears in (1) (see Newland, 1993a). When $f(\tau)$ correlates with $w^*(\tau-t)$, then $a(t)$ will be large; when they do not correlate, $a(t)$ will be small. More information is obtained if the process is repeated with a different wavelet function, $w_1(t)$. Any basis functions $w(t)$ can be used but to be a good method of identifying time-frequency distributions, it is

necessary to choose windowed harmonic functions with strong (i.e. localised) frequency content. Harmonic wavelets have this property. They are easy to use and have important advantages for vibration analysis when detailed time-frequency maps are required.

One advantage is their simplicity in the frequency domain. The algorithm illustrated in figure 1 begins by converting (1) from the time domain by taking Fourier transforms to give (see for example Newland, 1989, ch. 9)

$$A(\omega) = F(\omega)W^*(\omega) \tag{2}$$

where the quantitites shown with capital letters in (2) are the Fourier transforms of the corresponding quantities in (1). In order to make practical calculations, these Fourier transforms are computed by applying the FFT algorithm. It is a simple operation to compute the FFT of the input signal and it is then necessary to multiply this, term by term, by the complex conjugate of the FFT of the wavelet to be used. For the complex harmonic wavelet (Newland, 1993a, 1994a), the Fourier transform $W(\omega)$ is especially simple. It is zero everywhere except in a finite band of frequencies defined by

$$m2\pi \le \omega < n2\pi \tag{3}$$

where $m<n$ and need not be integers. Within this band it has the constant (real) value

$$W(\omega) = 1/\{(n-m)2\pi\}. \tag{4}$$

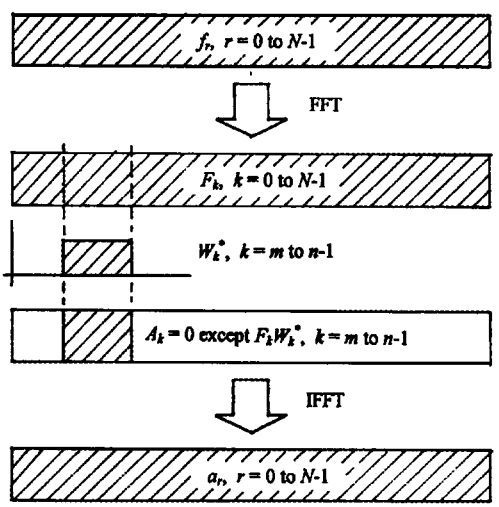

Figure 1. Harmonic wavelet transform used to compute the time-frequency distributions in this paper. The wavelet coefficients a_r define the distribution of (complex) amplitude in the frequency band $m2\pi \le \omega < n2\pi$ (for a record of unit length), from Newland (1997b).

Because the wavelets are complex, their Fourier transform is one-sided, so that $W(\omega)$ remains zero for all negative frequencies. For comparison, the algorithm of the orthogonal harmonic wavelet transform is shown in figure 2. For an input signal $f(t)$ which is sampled N times to give the sequence $f_0, f_1, f_2, \ldots f_{N-1}$, the algorithm in figure 2

produces *n-m* complex wavelet coefficients whose frequency is defined by the width of the block W_k^* (instead of N wavelet coefficients for the same block in figure 1). They are the result of making the correlation calculation in (4) for the centre of the wavelet $w_{m,n}(t)$ at each of *n-m* equally-spaced positions along the time axis.

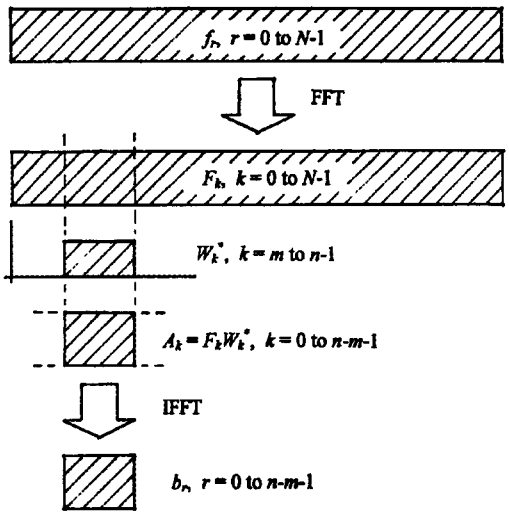

Figure 2. HWT algorithm for computing complex orthogonal wavelet coefficients for a time series of N real terms (from Newland, 1997a)

It is shown in the theory of harmonic wavelets that, if the calculation in figure 2 is repeated for all frequency blocks that cover the range 0 to the Nyquist frequency, with each block touching but not overlapping the next block, then a set of $N/2$ complex wavelet coefficients is generated that describes the amplitude and phase of a complete set of $N/2$ complex orthogonal harmonic wavelets.

A disadvantage of wavelets generated in this way is that their localisation in time is poor, with the envelope of the wavelets decreasing only in proportion to $1/t$. Localisation can be much improved by windowing the wavelet Fourier transform W_k^* before making the computation in figure 1. This destroys the orthogonality of the wavelets but much improves their ability to extract frequency data from the input signal. For signal deconstruction when it is desired to learn as much as possible about the content of a signal and reconstruction is not important, the loss of orthogonality is not important. Furthermore it has been found (Newland, 1997a,b) that the clarity of time-frequency maps generated by the HWT can be greatly improved by interpolating between the *n-m* wavelet coefficients computed in figure 2. This is what happens in figure 1. Instead of *n-m* coefficients, figure 1 generates N coefficients which are evenly spaced along the time axis at spacing $1/N$.

It can be shown (see, for example, Newland 1997b) that the Fourier coefficient r of an N term series will have the same magnitude as Fourier coefficient s of an *n-m* term series if

$$r / N = s / (n - m) \tag{5}$$

and they will have the same phase angle (ratio of imaginary to real part) if, in addition, m is zero (no leading zeros) or if

$$m / (n - m) = \text{any integer.} \tag{6}$$

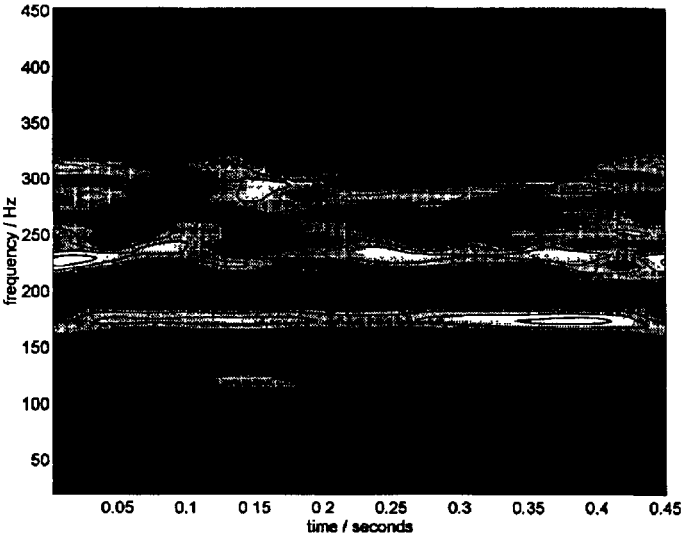

Figure 3. Harmonic wavelet map for the acceleration of a pump bearing.

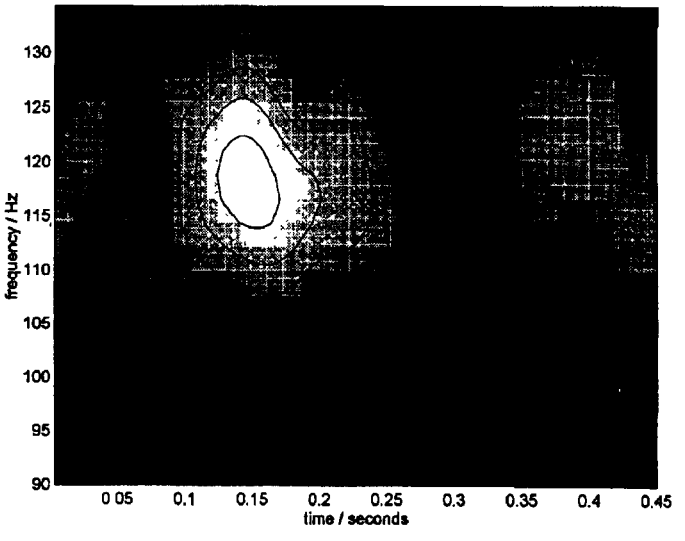

Figure 4. Zoom onto a small frequency slice through the map in figure 3.

The algorithm in figure 1 has been used for the examples shown below. For simplicity, each row of wavelet coefficients is computed for an N term series, with no leading zeros. Also each wavelet frequency band overlaps adjacent bands in order to improve frequency resolution. In this way, the energy of a signal is mapped into its frequency bands and contour or mesh diagrams can be generated to illustrate the distribution of either its

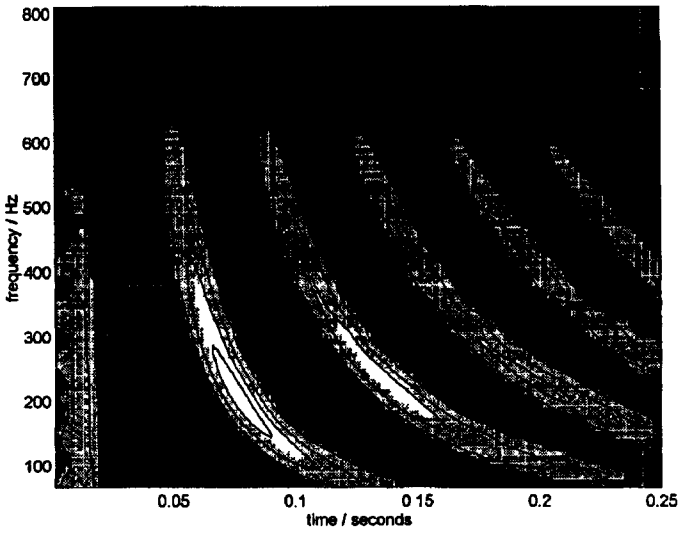

(a)

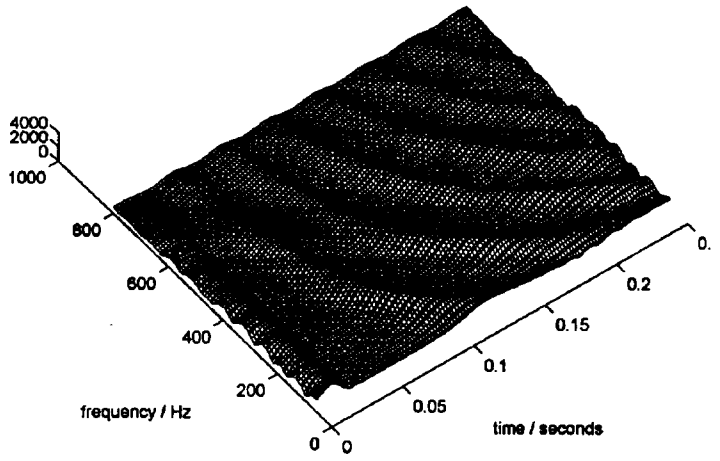

(b)

Figure 5. Harmonic wavelet map of the impulse response of a beam: (a) amplitude map, (b) corresponding mesh diagram

amplitude (by plotting the modulus of the wavelet coefficients) or its phase (by plotting the ratio of the imaginary to the real part of the wavelet coefficients) over time and frequency. Programming has been done in the Matlab® language; program variables and commands given below are in Matlab.

VARIABLE Q PROPERTY

Because the frequency block defined by m and n in figure 1 can be chosen arbitrarily, the bandwidth of the harmonic wavelets can be chosen arbitrarily. Therefore the Q

factor of wavelets can be chosen to suit the signal being analysed. Furthermore the frequency step between one row of wavelets and the next row can be chosen arbitrarily. Generally it is found helpful to overlap frequency bands, so that the frequency step is a small proportion of the bandwidth because this improves the resolution of the resulting time-frequency map. Also computations do not need to cover the full frequency range of

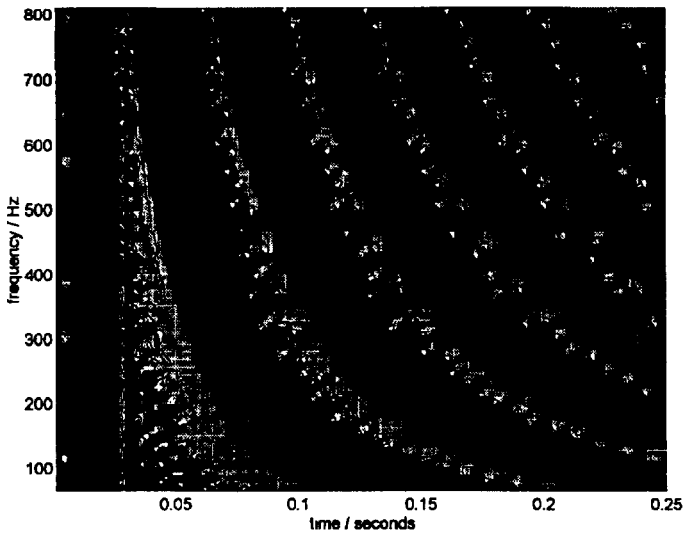

(a)

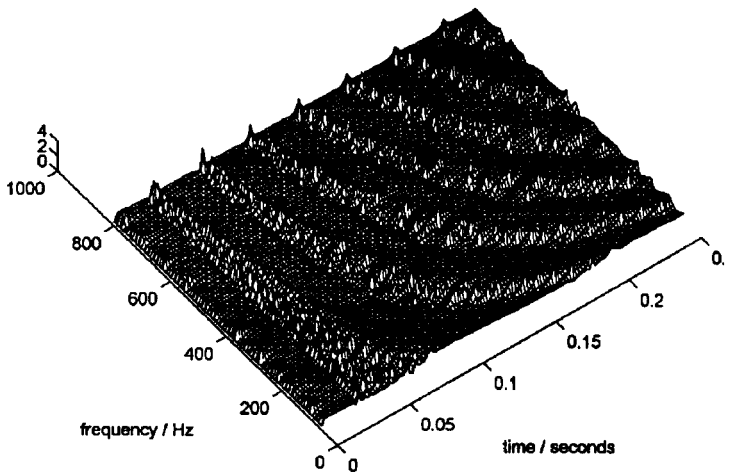

(b)

Figure 6. Harmonic wavelet maps of the impulse response of a beam: (a) differential phase map, (b) corresponding mesh diagram

the signal (i.e. zero frequency to the Nyquist frequency) as they have to for the STFT. If only a small range of frequencies is of interest, calculations need only be made for that range. An example is given below.

Figures 3 and 4 are for a measured record of vibration. It is data provided by the Kennedy Space Center and comes from one of the bearings of a liquid oxygen pump at the launch equipment test facility for the Space Shuttle. The pump's shaft rotational

speed is 57.5 Hz (3,450 rpm) and the acceleration has been measured in g's over a frequency range covered by the sampling frequency of 9,094 Hz. The data for figures 3 and 4 (and for all subequent figures) is included in table 1 below.

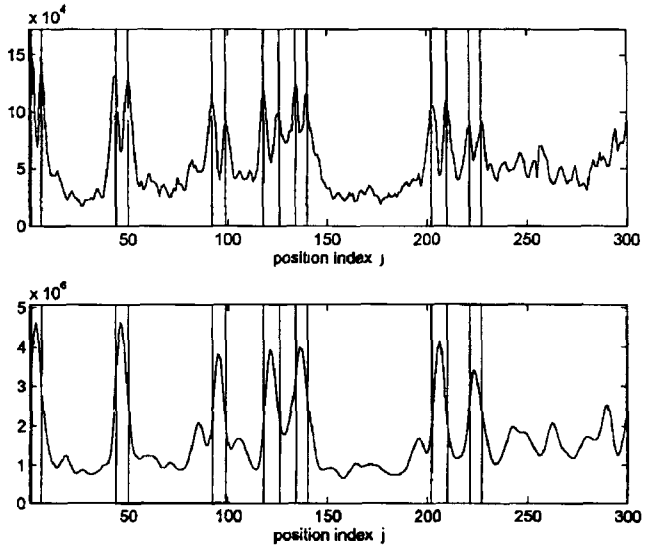

(a) above and (b) below

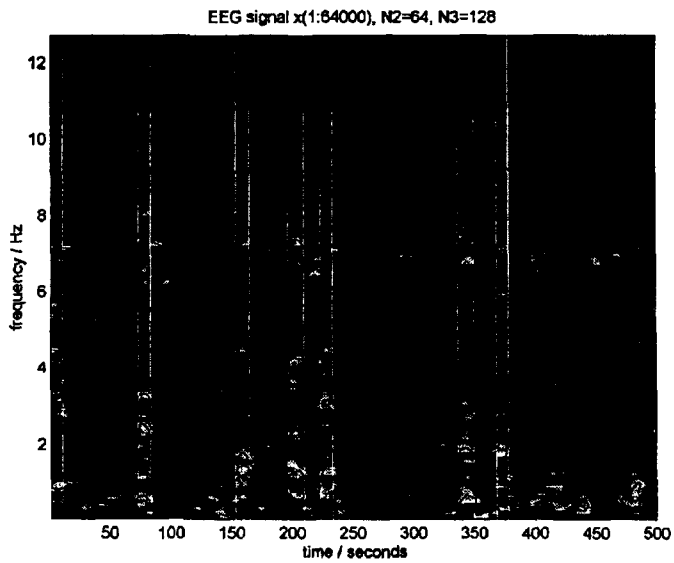

(c)

Figure 7. Segmentation of an EEG recording based on peaks in d(j)=sum((abs(A(:,j))-abs(A(:,j-1)).^2): (a) graph of discriminator d(j), (b) sum(abs(A(:,j).^2) for comparison, (c) map of abs(A(j,k)) with segment markers superimposed

The rectangular "tiles" on the right-hand side of the figures define the frerquency and time resolution of the map as described in a previous paper (Newland, 1997b). The map in figure 4 is a zoom onto a short section of the frequency axis. This is obtained by taking the IFFT (figure 1) only for frequency blocks in the vicinity of the second harmonic of

shaft speed. Although the transform seeks N4=128 frequency steps in the range from 90 to 135 Hz (see table 1), only about 20 steps are possible because it is only possible to move the frequency block in single integer steps.

PHASE MAPPING

An example used by the author before is for the measured acceleration of a suspended elastic beam (Newland, 1997a,b). When tapped at one end by a hammer with a soft tip

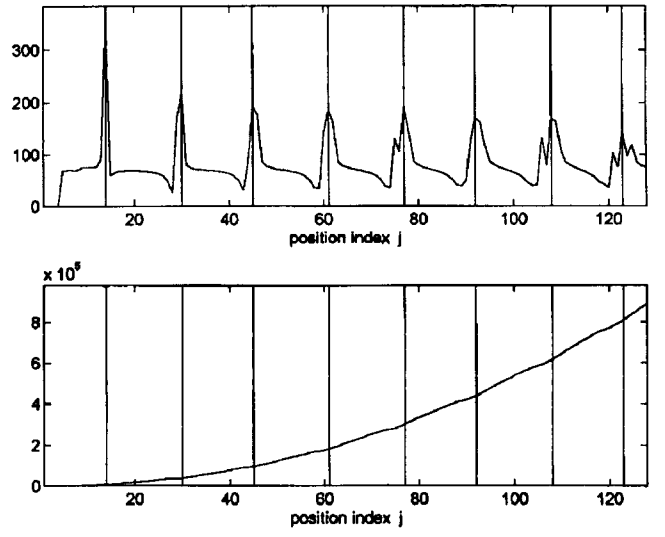

(a) above, (b) below

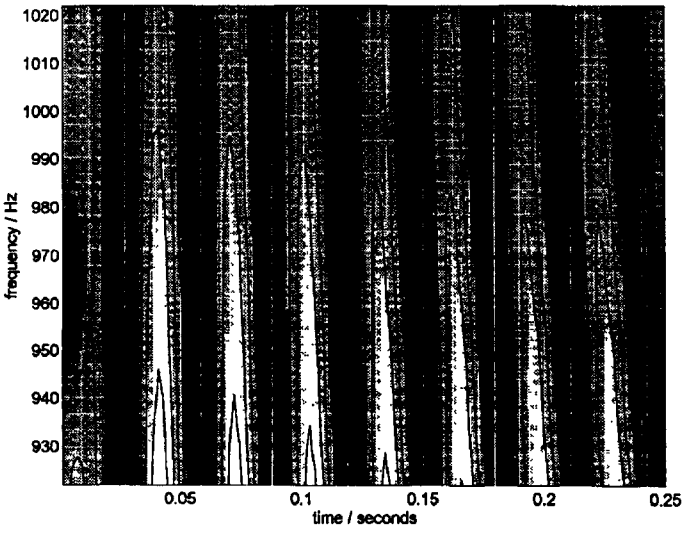

(c)

Figure 8. Segmentation of an EEG recording based on peaks in d(j)=sum((angle(A(:,j))-angle(A(:,j-1))).^2): (a) graph of discriminator d(j), (b) sum((angle(A(:,j)).^2) for comparison, (c) map of abs(A(j,k)) with segment markers superimposed

bending waves are generated which travel backwards and forwards along the beam, being detected in bursts at the measuring point. However because the system is dispersive, waves of different frequency travel at different speed. Therefore the measured time response records a jumble of waves and individual packets of waves cannot be identified. Figure 5 is a time-frequency map of wavelet amplitude, which is a measure of the distribution of mean-square signal over time and frequency.

In contrast, figure 6 is a plot of differential phase. It is not hepful to plot absolute phase because this describes the phase of the wavelet amplitudes at the reference positions of the wavelets. That depends on the (arbitrary) positions of the reference wavelets. Instead wavelet difference, for example abs(angle(A(j,k))-angle(A(j,k-1))), where A(:,:) is the time-frequency array, is plotted. During the bursts of energy when packets of travelling waves are being detected, there is a steady change of phase and so the differential phase is small. During lulls between these bursts, the phase fluctuates quite widely and so the differential phase is high with significant changes from column to column. The interpretation of differential phase diagrams is a subject of our continuing research at the present time.

SEGMENTATION BY AMPLITUDE

Figure 7 is an EEG signal kindly supplied by Prof. A. Procházka in which significant brain activity is being recorded for limited spells during an otherwise quieter period of about 500 seconds. A time-frequency map of wavelet amplitude is shown in figure 7(c). The top graph, figure 7(a), is a function defined as w(j)=sum((abs(A(:,j))-abs(A(:,j-1))).^2). This represents the sum over rows (frequency) of the squares of the differences between amplitudes from one column to the next (that is, from one time position to the next). The middle graph, figure 7(b), plots sum(abs(A(:,j)).^2), for comparison. The vertical lines identify peaks in the top graph and these have been projected down to the time-frequency map below, thereby segmenting the record into different spectral features. The sharp peaks in w(j) appear to be a good indicator of sudden changes in brain activity.

	Fig. 3	Fig. 4	Fig. 5	Fig. 6	Fig. 7	Fig. 8
Input sequence length (N) :	4,096	4,096	1,024	1,024	64,000	1,024
Output sequence length (N1):	256	256	128	128	128	128
Min. Fourier block length (N2):	16	16	32	32	64	32
Max. Fourier block length (N3):	16	16	32	32	128	32
Number of frequency levels (N4):	128	128	128	128	300	128
Lowest frequency, Nyquist*startf where startf =	0	0.02	0	0	0	0.45
Highest frequency, Nyquist*endf, where endf =	0.1	0.03	0.4	0.4	0.2	0.50
Window : Hanning, full block width						
Sampling frequency (sfreq, Hz)	9,094	9,094	4,096	4,096	128	4,096
Parameter plotted	abs (A(j,k))	abs (A(j,k))	abs (A(j,k))	abs angle difference	abs (A(j,k))	abs (A(j,k))
Contours at 10%, 30%, 50%, 70% and 90% of	max (abs(A))	max (abs(A))	max (abs(A))	max of array	max (abs(A))	max (abs(A))

Table 1. Numerical parameter values for the graphs plotted above

SEGMENTATION BY PHASE

The same method may be applied to differential phase by using an array matrix with wavelet phase having replaced wavelet amplitude. When applied to the beam impulse example described above, the result is shown in figure 8. Only a limited frequency span is used covering the range 930 to 1020 Hz. The top graph, figure 8(a), shows very distinct peaks of phase change at specific times. When these are projected down onto the amplitude time-frequency map below, it can be seen that they fall almost exactly at the middle of the valleys between the arrival of bursts of reflected energy of bending waves.

REFERENCES

Cohen, L., 1995, *Time-Frequency Analysis*, Prentice Hall, New Jersey.

Hammond, J. (editor), 1997, "Time-Frequency Methods - Special Issue," *Mechanical Systems and Signal Processing*, **11**, 507-650.

Hodges, C.H., Power, J. and Woodhouse, J., 1985, "The Use of the Sonogram in Structural Acoustics and an Applic-ation to the Vibrations of Cylindrical Shells," *J.Sound Vib.*, **101**, 203-218.

Mark, W. D., 1970, "Spectral analysis of the convolution and filtering of non-stationary stochastic processes," *J. Sound Vib.*, **11**, 9-63.

Newland, D. E., 1989, *Mechanical Vibration Analysis and Computation*, Addison Wesley Longman.

Newland, D. E., 1993a, "Harmonic Wavelet Analysis," *Proc. R.. Soc. Lond. A*, **443**, 203-225.

Newland, D. E., 1993b, *Random Vibrations, Spectral and Wavelet Analysis*, 3rd edition, Addison Wesley Longman.

Newland, D. E., 1994a, "Harmonic and Musical Wave-lets," *Proc. R. Soc. Lond. A*, **444**, 605-620.

Newland, D. E., 1994b, "Wavelet Analysis of Vibration, Part 1: Theory," *J. Vibration & Acoustics, Trans. ASME*, **116**, 409-416.

Newland, D. E., 1994c, "Wavelet Analysis of Vibration, Part 2: Wavelet Maps," *J. Vibration & Acoustics, Trans.ASME*, **116**, 417-425.

Newland, D. E., 1994d, "Wavelet Theory and Applic-ations," *Proc. 3rd Int. Congress on Sound and Vibration*, Montreal, Canada, 695-713 (Int. Science Publications, AL, USA). Reprinted as "Wavelet Analysis of Vibration Signals, Part 1" in *Int. J. Acoustics and Vib.*, **1**, 11-16, 1997.

Newland, D. E., 1996, "Time-Frequency Analysis by Harmonic Wavelets and by the Short-Time Fourier transform", *Proc. 4th Int. Congress on Sound and Vibration*, St. Peters-burg, Russia, 1975-82 (Int. Science Publications, AL, USA). Reprinted as "Wavelet Analysis of Vibration Signals, Part 2" in *Int. J. Acoustics and Vib.*, **1**, 1997.

Newland, D. E., 1997a, "Time-Frequency and Time-Scale Analysis by Harmonic Wavelets," *Proc. 1st European Conf. on Signal Analysis and Prediction*, Prague.

Newland, D. E., 1997b, "Practical signal analysis: do wavelets make any difference?", Paper DETC97/VIB-4135, *16th ASME Biennial Conf. on Vibration and Noise, Proc. 1997 ASME Design Engineering Technical Conferences* (CD ROM), Sacramento, California.